Experimental Neurology 296 (2017) 23–31

Contents lists available at ScienceDirect

Experimental Neurology

journal homepage: www.elsevier.com/locate/yexnr

Research Paper

Evidence that activation of P2X7R does not exacerbate neuronal death after optic nerve transection and focal cerebral ischemia in mice

Berrak Caglayan [a,b,e], Ahmet B. Caglayan [a,b], Mustafa C. Beker [a,b], Esra Yalcin [a,b], Merve Beker [c], Taha Kelestemur [a,b], Elif Sertel [a,b], Gürkan Ozturk [a,b], Ulkan Kilic [a,d], Fikrettin Sahin [e], Ertugrul Kilic [a,b,*]

[a] Istanbul Medipol University, Regenerative and Restorative Medical Research Center, Istanbul, Turkey
[b] Istanbul Medipol University, Dept. of Physiology, Istanbul, Turkey
[c] Bezmialem Vakif University, Dept. of Medical Biology, Istanbul, Turkey
[d] Istanbul Medipol University, Medical Biology, Istanbul, Turkey
[e] Yeditepe University, Dept. of Genetics and Bioengineering, Istanbul, Turkey

ARTICLE INFO

Article history:
Received 20 March 2017
Received in revised form 1 June 2017
Accepted 29 June 2017
Available online 29 June 2017

Keywords:
P2X7 receptor
Neuronal survival
Signaling
Cerebral ischemia
Optic nerve transection

ABSTRACT

Conflicting data in the literature about the function of P2X7R in survival following ischemia necessitates the conductance of in-depth studies. To investigate the impacts of activation vs inhibition of the receptor on neuronal survival as well as the downstream signaling cascades, in addition to optic nerve transection (ONT), 30 min and 90 min of middle cerebral artery occlusion (MCAo) models were performed in mice. Intracellular calcium levels were assessed in primary cortical neuron cultures. Here, we show that P2X7R antagonist Brilliant Blue G (BBG) decreased DNA fragmentation, infarct volume, brain swelling, neurological deficit scores and activation of microglial cells after focal cerebral ischemia. BBG also significantly increased the number of surviving retinal ganglion cells (RGCs) after ONT and the number of surviving neurons following MCAo. Importantly, receptor agonist BzATP resulted in increased activation of microglial cells and induced phosphorylation of ERK, AKT and JNK. These results indicated that inhibition of P2X7R with BBG promoted neuronal survival, not through the activation of survival kinase pathways, but possibly by improved intracellular Ca^{2+} overload and decreased the levels of Caspase 1, IL-1β and Bax proteins. On the other hand, BzATP-mediated increased number of activated microglia and increased survival kinase levels in addition to increased caspase-1 and IL-1β levels indicate the complex nature of the P2X7 receptor-mediated signaling in neuronal injury.

1. Introduction

P2X7 receptors (P2X7R) are ligand gated ionotropic channels that are located on the cell membrane and, upon activation, responsible for facilitating the cationic currents into the cell (North, 2002; Khakh and North, 2006; Murrell-Lagnado and Qureshi, 2008). These ATP sensitive homomeric receptors belong to purinergic P2X receptor family and have recently gained particular importance as a target in pharmacotherapies due to their pathophysiological functions in the central nervous system (CNS) (Burnstock, 2007; North and Jarvis, 2013).

In case of a cellular injury, large amounts of ATP are released from the cell. Upon ATP binding, P2X7R channel shifts to an open state allowing the passage of small cations, such as Na^+, K^+ and Ca^{2+}. The sustained activation of the receptor and maintenance of its open state for a prolonged period of time eventually result in membrane blebbing and cell death (Skaper et al., 2010). On the other hand, numerous findings indicate P2X7Rs' neuroprotective effect in CNS pathologies (Bindra et al., 2014; Suzuki et al., 2004; Yanagisawa et al., 2008). These two-sided evidences along with the critical roles that P2X7R plays in pathophysiology of Alzheimer disease (Diaz-Hernandez et al., 2012), Parkinson's disease (Marcellino et al., 2010), retinal diseases (Zhang et al., 2005) as well as cerebral ischemia (Bai and Li, 2013) increase the need for clarifying its physiological properties, especially in the CNS.

On the other hand, ischemic stroke is the most frequently encountered stroke subtype in adults worldwide. In the US, it is stated to be the third cause of death; it is also known to cause long-term disability. Yet, there is no effective treatment available except from tissue plasminogen activator which has a time limitation (Thrift et al., 2014; Mathers et al., 2009). The surrounding neuronal tissue around the affected core is lost soon after the occlusion, while the cellular damage in so-called penumbra still appears to be reversible. Meanwhile, necrotic cell death provides an extensive source of extracellular ATP, which in return activates P2X7 receptors and subsequent signaling cascades that will

* Corresponding author at: Department of Physiology, Istanbul Medipol University, Regenerative and Restorative Medical Research Center, Ekinciler cad. 19, TR-34810 Istanbul, Turkey.
E-mail address: ekilic@medipol.edu.tr (E. Kilic).

http://dx.doi.org/10.1016/j.expneurol.2017.06.024
0014-4886/

help defining the fate of the cell along with the other pathophysiological events of the ischemic brain (Diaz-Hernandez et al., 2012; Dirnagl et al., 1999).

Moreover, retina is considered as an extension of the CNS and manifests similar pathophysiological processes in neurodegenerative disorders to that of brain and spinal cord (Dirnagl et al., 1999; London et al., 2013). Degenerative process in retina lasts a prolonged time period compared to the CNS, providing researchers a broadened timeframe to understand the entire process through noninvasive monitoring methods as well as to prevent the unwanted outcomes of the pathological environment (London et al., 2013).

To this end, the present study has been carried out to investigate the involvement of activation and inhibition of P2X7 purinergic receptors in in vivo acute and sub-acute ischemic injury as well as in retinal injury models. By doing so, we aimed to define the signaling pathways and molecular mechanisms to provide a clearer understanding to the controversial role of P2X7R in the CNS.

2. Material and methods

2.1. Animals and experimental procedures

All experimental procedures were carried out with government approval according to NIH guidelines for the care and use of laboratory animals. Ethical committee approval was obtained from Istanbul Medipol University. In this study, adult male C57BL/6j mice weighing 22–26 g were randomly assigned to one of four groups and subjected to 30 min or 90 min of focal cerebral ischemia (FCI). Animals were anesthetized with 1% isoflurane (30% O_2, remainder N_2O) and then; 1) vehicle (isotonic saline), 2) Brilliant Blue G (BBG), 3) Benzoylbenzoyl ATP triethylammonium salt (BzATP) or 4) both BBG and BzATP (n = 7 for all groups) was carefully injected intracerebroventricularly (i.c.v.). Thirty minutes after the i.c.v. injections, animals were submitted to 30 min or 90 min of MCA occlusions, according to the procedure described below. For optic nerve transection, adult male C57BL/6j mice weighing 22–26 g were randomly assigned to one of four groups as stated before.

2.2. Transient focal cerebral ischemia

Animals (9–11 weeks) were anesthetized with 1% isoflurane (30% O_2, remainder N_2O). Body temperature was maintained between 36.5 and 37.0 °C using a feedback-controlled heating system. During the experiments, cerebral blood flow (CBF) was measured using a laser Doppler flowmetry (LDF) with a flexible 0.5 mm fiber optic probe (Perimed), which was attached to the intact skull overlying the middle cerebral artery (MCA) territory (2 mm posterior/6 mm lateral from bregma). LDF changes were monitored up to 30 min after the onset of reperfusion. Focal ischemia was induced using an intraluminal filament technique (Wang et al., 2005; E. Kilic et al., 2006; U. Kilic et al., 2006). Either 30 min or 90 min after MCA occlusions (MCAo), reperfusion was initiated by withdrawal of the monofilament. Anesthesia was discontinued and animals were placed back into their cages. Twenty-four hours (for 90 min of MCAo) or 72 h (for 30 min of MCAo) later, animals were deeply re-anesthetized and decapitated.

2.3. I.c.v. injections

Either 1) vehicle (saline), 2) 10 μg BBG (Santa Cruz Technologies, sc-203733), 3) 5 μg BzATP (Santa Cruz Technologies, sc-203862) or 4) both BBG and BzATP were i.c.v. injected in 2 μl volume for a total of 2 min duration. Thirty min after the injections, animals were submitted to MCAo, as described in Section 2.2.

2.4. Infarct volume and brain edema

Brain sections were fixed and stained with cresyl violet. For assessment of infarct volume and brain edema, a total of four sections from equidistant brain levels, 2 mm apart, were analyzed (sections selected starting from the rostral pole of the striatum: bregma +2.0 mm, subsequent sections taken from bregma 0.0, −2.0 and −4.0 mm). On these sections, brain infarcts were outlined by delineating non-lesioned tissue in both hemispheres, from which edema-corrected infarct areas and infarct volumes were calculated. Brain edema was analyzed by outlining lesioned and nonlesioned tissue in both hemispheres, which were subtracted from each other and divided by the non-lesioned tissue in the contralateral brain, thus calculating percentage values of brain swelling.

2.5. Analysis of neuronal survival and immunofluorescence

Adjacent brain sections of the same animals were fixed in 4% paraformaldehyde (PFA)/0.1 mol/l phosphate buffered saline (PBS), washed and immersed for 1 h in 0.1 mol/l PBS containing 0.3% Triton X-100 (PBS-T)/10% normal goat serum. Sections were incubated overnight at 4 °C with Alexa Fluor 488-conjugated monoclonal mouse anti-NeuN (Mab377X; Chemicon). Next day, sections were incubated with 4′,6-diamidino-2-phenylindole (DAPI). Sections were analyzed using a confocal Zeiss LSM 780 microscope (Carl Zeiss, Jena, Germany). Nine different region of interest (ROI) in the striatum, each measuring 62,500 μm^2, were evaluated. Mean numbers of NeuN cells were analyzed in the ischemic and contralesional striatum. By dividing results obtained in both hemispheres, the percentage of surviving neurons in the ischemic striatum was determined.

For immunofluorescence analysis of Iba1+ cells, brain sections of animals submitted to 30 min ischemia and 72 h reperfusion were prepared for the following groups: 1) vehicle (isotonic saline), 2) BBG, 3) BzATP or 4) both BBG and BzATP. Sections were fixed with ice cold acetone at −20 °C for 10 min, blocked with 10% normal goat serum/PBS containing 0.3% Triton X-100 and incubated overnight at 4 °C with anti-Iba1 antibody (019-19741, Wako). On the next day, secondary antibody (Alexa Fluor-488 conjugated goat anti-rabbit, A-11034, Invitrogen) was incubated for 1 h and finally, sections were treated with DAPI as a counterstaining and imaged with LSM 780 microscope (Carl Zeiss, Jena, Germany). Nine different region of interest (ROI) in the ischemic striatum, each measuring 62,500 μm^2, were evaluated. Numbers of Iba-1+ cells were counted.

2.6. DNA fragmentation

From animals subjected to 30 min MCAo, sections from the level of the mid-striatum (bregma 0.0 mm) were stained with terminal transferase biotinylated-dUTP nick end labeling (TUNEL) assay using a commercially available kit (In situ cell death Roche) (E. Kilic et al., 2006; U. Kilic et al., 2006). In these sections, DNA-fragmented cells were counted in a blinded manner in the same nine random regions of interest (ROI) in the striatum (each 62.500 μm^2) as above.

2.7. Western blot

Tissue samples were obtained from ischemic striatum and overlying cortex and Western blot analyses were carried out as described previously in Beker et al., 2015 with minor modifications. Samples of the same group were pooled, homogenized in the lysis buffer containing protease/phosphatase inhibitor cocktail (5872, Cell Signaling) and equal amounts of protein (20 μg) were size-fractionated by 4–12% NuPAGE electrophoresis, transferred to polyvinylidene fluoride membrane (PVDF) using iBlot Dry Blotting System (Invitrogen). Membranes were blocked in blocking solution (5% non-fat milk in 50 mM Tris-buffered saline containing 0.1% Tween, TBS-T), incubated overnight

with pAKT (4060; Cell Signaling), pERK-1/-2 (9101; Cell Signaling), pJNK-1/-2 (9255; Cell Signaling), IL-1β, (ab9722; Abcam), Bax, (2772; Cell Signaling), Bcl-xL, (2764; Cell Signaling), Cleaved caspase-1 (22165, Santa Cruz), and P2X7R (106246; Abcam). Protein loading was controlled by stripping and reprobing the blots with β-actin antibody (4967, Cell Signaling). Blots were developed using ECL-Advanced Western Blotting Detection Kit (Amersham, GE Health Care) and visualized by the MF-ChemiBIS (DNR). Intensity of each signal was measured on a total of three digitized blots each using the Image J software program. Protein levels were analyzed densitometrically and corrected with values determined on β-actin blots.

2.8. Culture of primary cortical neurons

Cultures of primary cortical neurons were prepared from brain cortices of P0-P3 C57BL/6j mice by brief modification of the protocol described before (Hilgenberg and Smith, 2007). Briefly, cortical tissue was papain (P4762; Sigma) digested after dissection, gently triturated and seeded onto poly-D lysine coated 35 mm glass-bottom petri plates. Cultures were incubated at 37 °C in a humidified atmosphere of 95% air and 5% CO_2 in Neurobasal A medium (10888-022; Gibco) supplemented with 2% B27 (17504-044; Gibco), 1% GlutaMax-1 (3503-039; Gibco) and 1% antibiotic and antimycotic solution (450115-E2; MultiCell). Culture medium was refreshed in every 2 days and cells of 5–7 days in vitro (DIV) were used in experiments.

2.9. Calcium imaging

Calcium imaging was performed as described before (Barreto-Chang and Dolmetsch, 2009). Briefly, when cells reached DIV7, cells were washed with Hank's Balanced Salt Solution (HBSS) and loaded with 5 μM Fura 2-AM (F0918; Sigma). After 30 min of incubation at 37 °C, plates were washed with HBSS and fresh medium was added, and images were taken with spinning disk microscope (Zeiss Cell Observer Spinning Disk Confocal). Fluorescent measurements at 463 nm emission were taken as the ratio of the signals obtained upon excitation by 340/380 nm. Time lapse records of the first 10 min were taken as baseline and used to normalize the data obtained at designated time points. Eight different regions of interest (ROI) and five cells in each ROI were analyzed per each group. At the end of the measurements, cells were fixed with 4% PFA and stained with NeuN.

2.10. Retrograde labeling of retinal ganglion cells (RGCs) and optic nerve (ON) transection

Retrograde labeling of RGCs were performed according to the protocol described before (E. Kilic et al., 2006; U. Kilic et al., 2006; Kilic et al., 2008). Briefly, 0.7 μl fluorogold (infusion rate 0.7 μl/min) was injected stereotactically into both superior colliculi. After infusion, the injection needle remained inside the tissue for 2 min before the syringe was withdrawn. Four days after labeling, right ON was transected approximately 0.5 mm distant to the posterior pole of the eye. Wounds were sutured and the retinal blood supply was verified by fundoscopy (E. Kilic et al., 2006; U. Kilic et al., 2006).

2.11. Intraocular injections

By means of a glass microelectrode with a tip outer diameter of 50 μm, 1 μl of either i) Vehicle, ii) 10 mM BBG, iii) 250 μM BzATP or iv) combination of BBG and BzATP was carefully injected into the vitreous space, puncturing the eye at the cornea-sclera junction (n = 7 animals/group). Injections were done at Day 0, 4, 7, and 10 after optic nerve transection as described above. Fourteen days after ON transection, mice were sacrificed and both eyes were removed. Retinas were dissected, flat-mounted on glass slides, and fixed in 4% PFA in 0.1 M phosphate-buffered saline (PBS) for 30 min.

2.12. Evaluation of RGC survival by stereology of surviving RGCs

Surviving RGCs were evaluated by confocal microscope (Zeiss, LSM-780) in retinal whole-mounts. RGC densities were determined by counting tracer-labeled RGCs in 12 random ROI (three areas per retinal quadrant at different eccentricities of 1/6, 3/6 and 5/6 of the retinal radius, respectively; measuring 62.500 μm^2 each) (E. Kilic et al., 2006; U. Kilic et al., 2006). Mean values were calculated for all eccentricities as well as over the whole retina.

2.13. Statistical analyses

Data were analyzed by oneway ANOVA followed by least significant differences (LSD) tests by using SPSS for Windows 18. For the evaluation of calcium imaging repeated measurement ANOVA were used (comparisons between independent groups elucidating interactions for calcium imaging). All values are given as mean ± S.D. with n values, indicating the number of different animals analyzed (n = 7–9 animals per group and 5 cells per fura analysis for each group). P values < 0.05 are considered significant.

3. Results

3.1. P2X7R antagonist BBG protects against 90 min of focal cerebral ischemia

Due to conflicting data in the literature about the role of P2X7R in ischemia, it was important to assess the receptor's function in depth. To investigate the changes in necrotic parameters following activation or inhibition of P2X7R in ischemia reperfusion (I/R) injury, a more severe I/R injury model consisting of 90 min of ischemia followed by 24 h reperfusion was chosen. We have previously shown that 90 min of MCAo model causes a focal infarct in the cerebral cortex as well as in the underlying striatum, and a subsequent edema (E. Kilic et al., 2006; U. Kilic et al., 2006). After reperfusion, CBF increased rapidly back to normal in all animals subjected to both 30 min and 90 min MCAo, with a slight, but not significant, upward shift in BBG (Fig. 1A). Infarct volume and brain swelling were assessed by cresyl violet staining of coronal sections. Infarct volume was significantly decreased (Fig. 1B), and brain swelling showed some, but not significant, decrease in BBG alone or BBG + BzATP administered groups (Fig. 1C). Neurological deficit scores were also significantly decreased in BBG or BBG + BzATP groups, indicating less severe consequences on motor neuron functions with P2X7R antagonism (Fig. 1D). Complete reversal of the unfavorable effect of BzATP with BBG raised the question whether the dosage used was not high enough. Therefore, we added a new BzATP group with the highest soluble in vivo dose possible. Interestingly, administration of even four fold higher dose (20 μg) did not worsen the outcomes when compared with vehicle or 5 μg BzATP group regarding infarct volume, brain swelling and neurological score values (Fig. 1B–D).

3.2. P2X7R antagonist BBG also protects against 30 min of focal cerebral ischemia

It has been reported that 30 min MCA occlusion induces selective neuronal injury in the striatum (Beker et al., 2015). In this model, LDF records exhibited a similar pattern in all animal groups (Fig. 2A). To determine the effects of P2X7R activation or inhibition on apoptotic cell death, DNA fragmentation was assessed with TUNEL staining. Number of TUNEL positive cells was decreased in BBG group (Fig. 2B). Neuronal survival, as evaluated by NeuN immunohistochemistry, was increased with BBG administration (Fig. 2C). BzATP did not significantly affect the number of DNA fragmented cells, but significantly decreased the number of surviving neurons (Fig. 2B, C). On the other hand, when given with BBG, it slightly reduced the favorable outcomes of BBG,

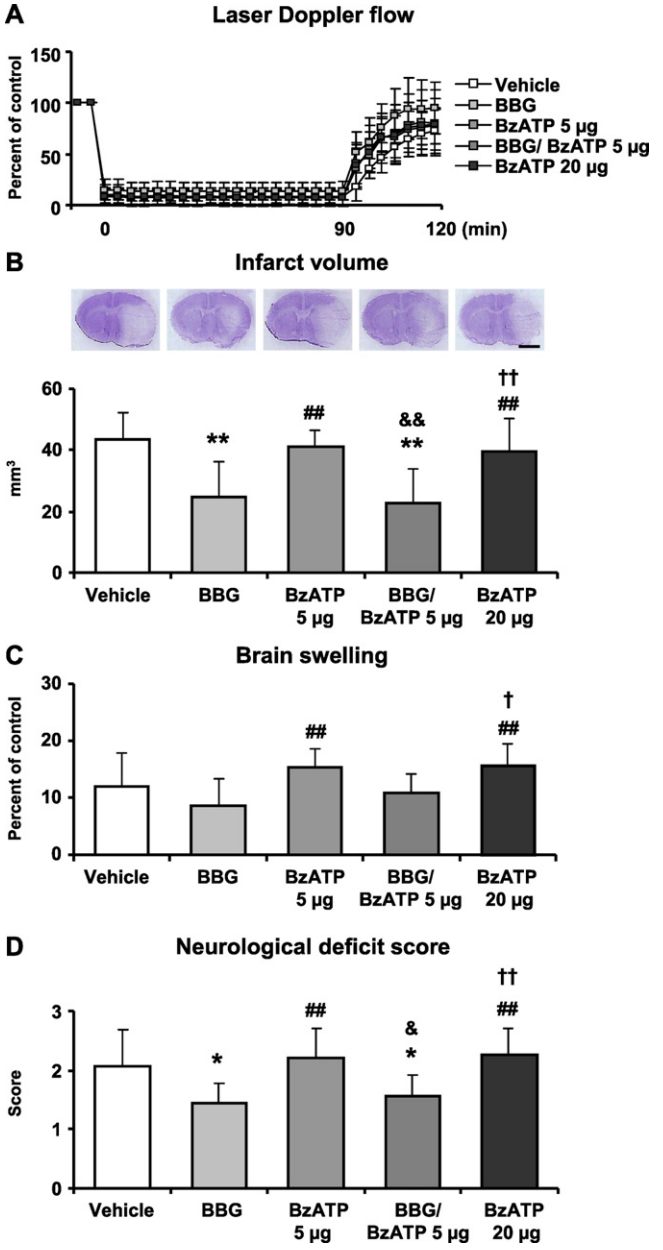

Fig. 1. P2X7R antagonist BBG protects against 90 min of focal cerebral ischemia. Cerebral blood flow during and after 90 min of intraluminal middle cerebral artery occlusion (MCAo) were recorded using Laser Doppler flowmetry (LDF) (A). Note that LDF values after reperfusion are moderately higher in animals receiving BBG. Infarct volume (B) and brain swelling (C) were analyzed 24 h after 90 min of MCAo in cresyl violet stained brain sections. Neurological deficit scores (D) were also evaluated 24 h after 90 min of MCAo. Data are mean values ± S.D. (n = 7 animals/group). $^{**}p < 0.01/^{*}p < 0.05$ compared with vehicle; $^{\#\#}p < 0.01$ compared with BBG treatment; $^{\&\&}p < 0.01/^{\&}p < 0.05$ compared with BzATP treatment; $^{\dagger\dagger}p < 0.01/^{\dagger}p < 0.05$ compared with BBG/BzATP 5 µg treatment. Scale bar equals to 2 mm.

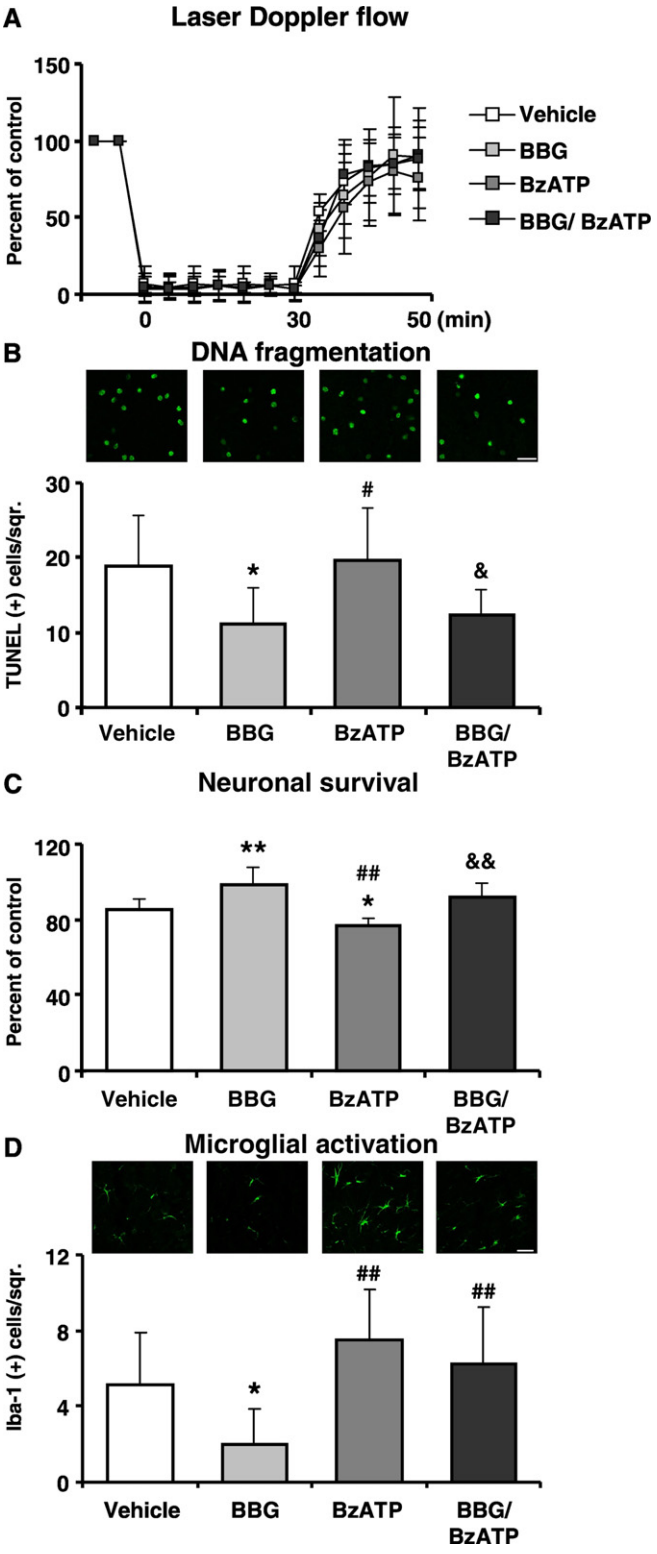

although not to a significant extent (Fig. 2B, C). This suggests that inhibition of P2X7R has an essential role in protection of neurons from the effects of ischemic insult. In addition, Iba1 immunopositive microglial cells were counted and analyzed for the groups: Vehicle (isotonic saline), BBG, BzATP and both. Data demonstrated that BzATP and BBG + BzATP significantly increased the number of Iba1+ cells in the ischemic striatum, when compared with BBG administered group. Additionally, BBG significantly decreased the number of Iba1+ cells when compared with control (Fig. 2D).

Fig. 2. P2X7R antagonist BBG protects against 30 min of focal cerebral ischemia. Laser Doppler flow (LDF) recordings during and after 30 min of intraluminal MCAo were similar with that of 90 min MCAo (A). DNA fragmentation (B), neuronal survival (C) and microglial activation/reaction (D) were evaluated 72 h after 30 min of MCAo. BBG significantly reduced the number of TUNEL+ and Iba-1 (+) microglial cells, which was associated with increased neuronal survival in the ischemic striatum. However, BzATP and vehicle did not show any difference in number of apoptotic cells, while activation of P2X7R by BzATP increased the number of activated microglial cells. Data are mean values ± S.D. (n = 7 animals/group). $^{**}p < 0.01/^{*}p < 0.05$ compared with vehicle; $^{\#\#}p < 0.01/^{\#}p < 0.05$ compared with BBG; $^{\&\&}p < 0.01/^{\&}p < 0.05$ compared with BzATP. Scale bar equals to 100 µm.

3.3. BzATP induces survival kinases

Our above results indicated P2X7R as a critical player in the ischemic neuronal death in mice. To further investigate the underlying mechanisms by which inhibition of this receptor promoted neuronal survival, we performed an extensive analysis of protein expression levels of survival and stress kinases as well as their downstream targets. First, levels of phosphorylated AKT (pAKT) and ERK1/2 (pERK-1/-2) were decreased in BBG treated groups, while elevated significantly with BzATP or BBG + BATP (Fig. 3B, C). Additionally, pJNK showed a significant increase only in the BzATP group, while being unchanged in BBG or BBG + BzATP groups (Fig. 3D).

3.4. BzATP induces expression of inflammation-related proteins

It was suggested that the expression of P2X7R was increased following an injury to the CNS (Rodrigues et al., 2015; Tewari and Seth, 2015), however the effects of its activator or inhibitor on the expression of the protein was not documented. Here, we evaluated the expression of P2X7R and showed that neither the activator, nor the inhibitor resulted in a significant change (Fig. 3E). Although BzATP decreased the expression slightly and such decrease would suggest a negative feedback loop, it was not significant. Upon activation, caspase-1 cleaves and activates the key pro-inflammatory cytokine IL-1β (Denes et al., 2012). To determine the effects of P2X7R on caspase-1 dependent inflammation

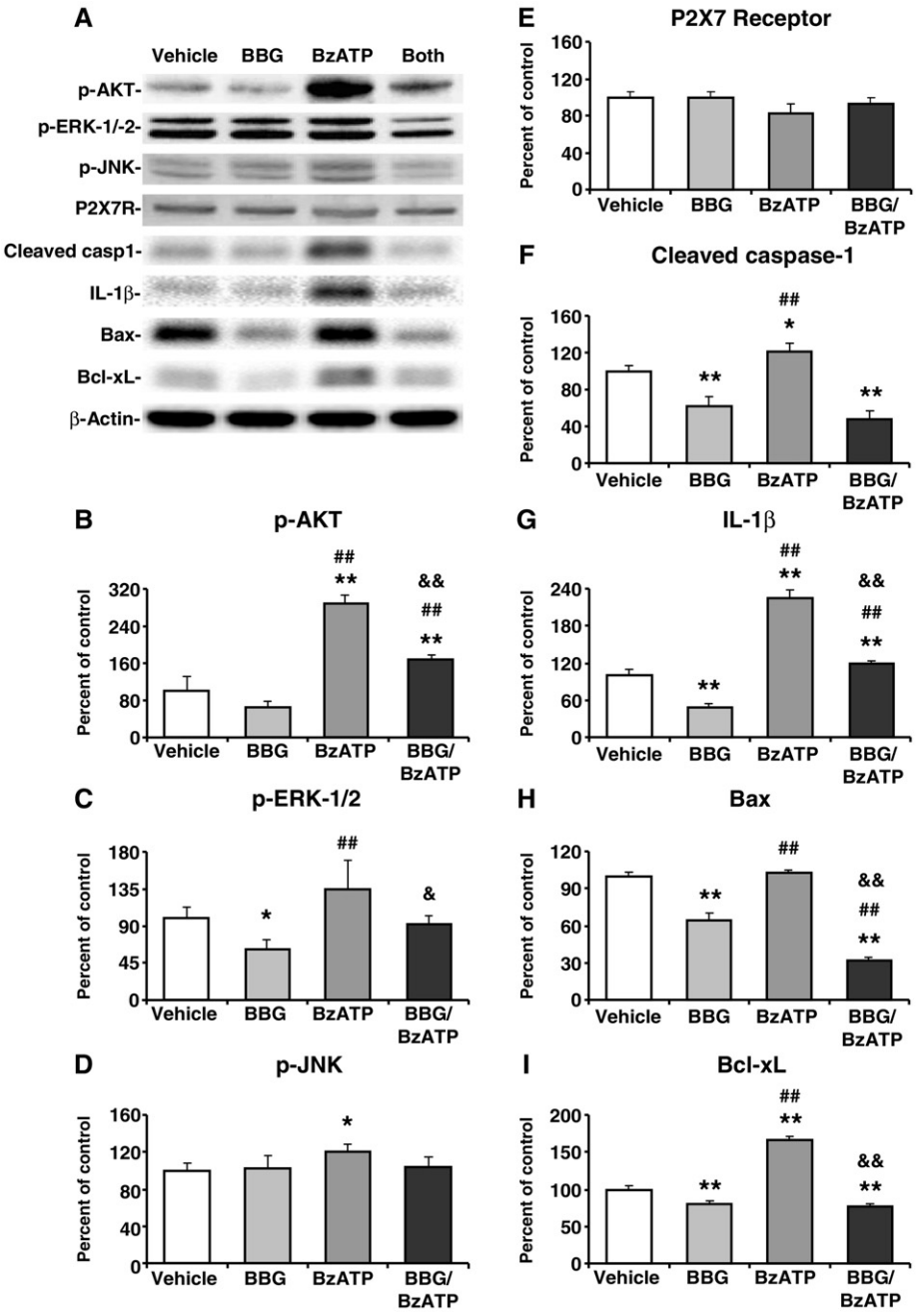

Fig. 3. Expressions of p-AKT, p-ERK-1/2, p-JNK, P2X7R, Cleaved caspase-1, IL-1β, Bax and Bcl-xL were demonstrated with Western blot (A). BzATP significantly increased p-AKT, p-GSK3, p-JNK, p-ERK-1/2, Cleaved caspase-1, IL-1β, Bax and Bcl-xL. On the other hand BBG significantly decreased p-ERK-1/2, Cleaved caspase-1, IL-1β, Bax and Bcl-xL. Data are mean values ± S.D. (n = 7 animals/group). $^{**}p < 0.01/^{*}p < 0.05$ compared with vehicle; $^{\#\#}p < 0.01$ compared with BBG treatment; $^{\&\&}p < 0.01/^{\&}p < 0.05$ compared with BzATP treatment.

mechanism, caspase-1 and IL-1β were evaluated. BzATP significantly increased these two proteins, while inhibition of the receptor resulted in a significant decrease (Fig. 3F, G). When given together with BzATP, BBG diminished the inflammatory response driven by the activation of the receptor. BBG when given alone or when given together with BzATP, significantly decreased Bax levels, while BzATP alone had no apparent effect on Bax levels (Fig. 3H). Surprisingly, BzATP significantly increased protein levels of anti-apoptotic Bcl-xL levels, although BBG resulted in a significant decrease (Fig. 3I).

3.5. BBG reduces intracellular Ca^{2+} overload

In this study, we observed that P2X7R antagonist BBG increased neuronal survival in both focal cerebral ischemia models in mice, while the agonist did not result in an opposite effect. Furthermore, a thorough analysis of the signaling pathways did not provide evidence supporting the protective mechanism observed with BBG. In fact, protein levels of survival-promoting pathways (such as, pAKT, pERK) were higher in the BzATP group. It is well-known for P2X receptors that once activated, they increase the mobility of intracellular Ca^{2+} levels. Therefore, we hypothesized that the mechanism accounted for improved neuronal survival through BBG-mediated P2X7R inhibition could be the intracellular Ca^{2+} homeostasis. We assessed this by measuring intracellular Ca^{2+} levels in vitro in primary cortical neurons subjected to glutamatergic toxicity (Fig. 4A). Glutamate excitotoxicity is one of the pathophysiological outcomes of ischemia/reperfusion injury in brain, which causes extensive Ca^{2+} influx and eventual cell death (Dirnagl et al., 1999). BBG reversed the increase in Ca^{2+} levels that were otherwise induced by glutamate. In comparison, BzATP resulted in a further increase in the amount of Ca^{2+} influx (Fig. 4B).

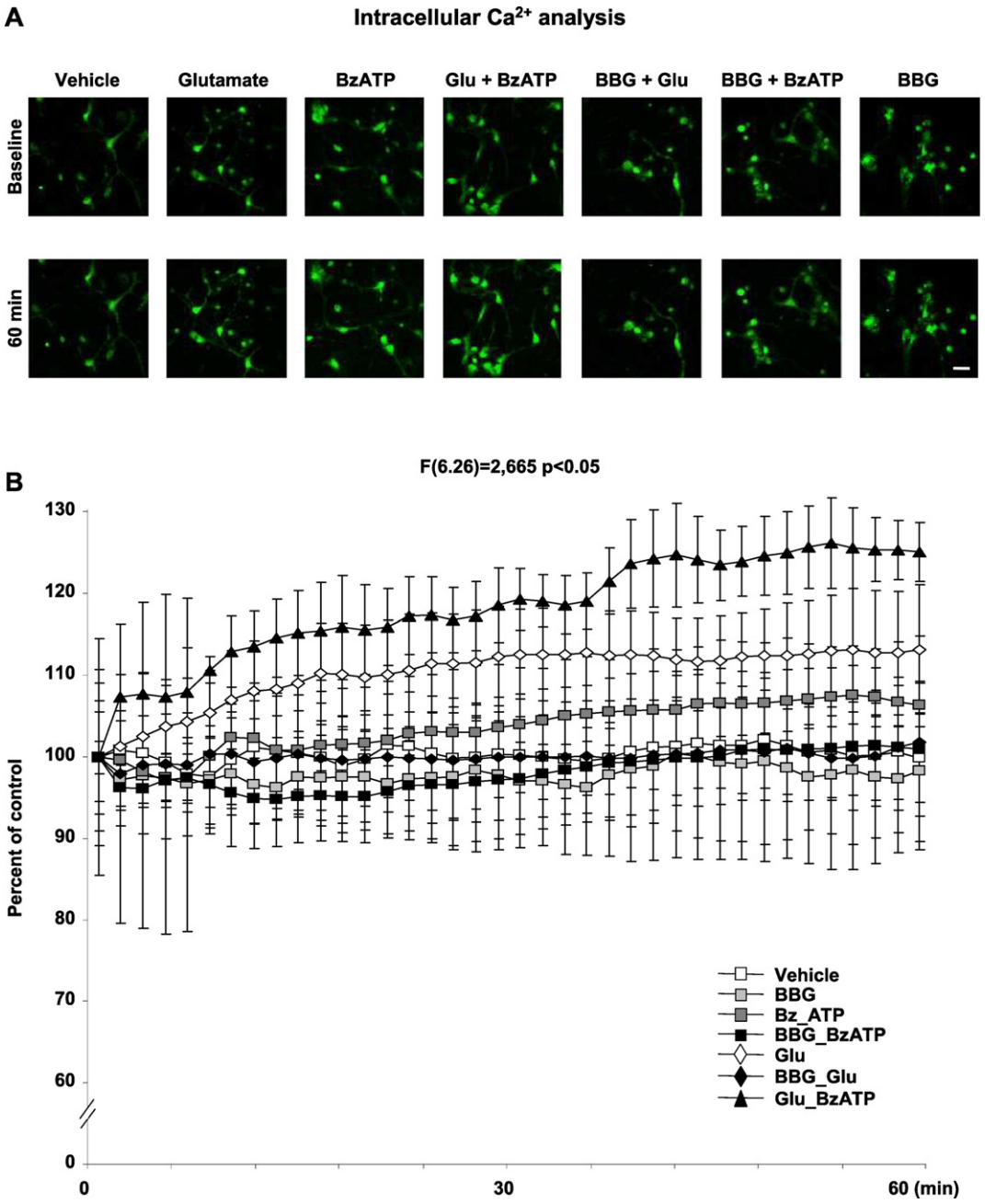

Fig. 4. Intracellular Ca^{2+} analysis of primary cortical culture. Cultures were imaged before (baseline) and after (60 min of treatment) (A). Intracellular Ca^{2+} load was assessed using Fura 2-AM and given as percent of control (B). In cultures subjected to glutamatergic toxicity, BzATP increased intracellular Ca^{2+} overload, while BBG had a complete reverse effect on intracellular Ca^{2+} load. Data are mean values ± S.E.M. (n = 5 cells/region in 8 different regions per sample). Scale bar equals to 50 μm.

3.6. P2X7R inhibition, but not activation, promotes survival of axotomized RGCs

We investigated the effect of P2X7R activation and inhibition on axotomized RGC survival by counting the number of Fluorogold pre-labeled RGCs. Application of a selective P2X7R antagonist BBG (10 mM) increased surviving RGCs significantly, compared with control or P2X7R agonist, BzATP (Fig. 5A). Albeit, application of BzATP (250 μM) did not further reduce the survival rate of these cells below the vehicle control. Moreover, when BzATP was applied together with BBG, it partially ceased the favorable effect of BBG in terms of number of RGCs in the axotomized retina. Survival rates were averaged for whole retina (Fig. 5A) and calculated separately for various (inner, middle and outer) retinal eccentricities as shown in Fig. 5B.

4. Discussion

The ongoing debate whether P2X7Rs have protective or degenerative effects on the expansion of central nervous system injuries was inconclusive at the time of the conductance of this study. P2X7R seems to display two opposing and contradictory functions in different experimental setups. The discrepancy among the reports in the literature may be due to the use of different animal species or strains or different models to mimic ischemic injury. Herein, the involvement of P2X7R in injury was studied in optic nerve (ON) transection and two ischemia/reperfusion injury models, in which 90 min of occlusion followed by 24 h reperfusion results in reproducible, large infarcts (E. Kilic et al., 2006; U. Kilic et al., 2006; Barreto-Chang and Dolmetsch, 2009; Gandelman et al., 2010), whereas 30 min of occlusion followed by 72 h reperfusion leads to selective neuronal injury (Wang et al., 2005; Kilic et al., 2008; Nagasawa et al., 2009). On the other hand, ON transection mimics delayed neurodegenerative processes, since it subsequently leads to degeneration of approximately 80% of RGCs within 14 days post-injury (E. Kilic et al., 2006; U. Kilic et al., 2006; Kilic et al., 2008). Presently, we report that inhibition of P2X7R using a potent and selective antagonist, BBG, promotes neuronal survival in all three models used. In line with our findings, in a unilateral optic nerve crush model using P2X7R knockout mice as well as pharmacological inhibition of P2X7R, delayed retinal ganglion cell death was observed (Nadal-Nicolás et al., 2016). In contrast, a study in genetically ablated P2X7R mice submitted to cerebral ischemia, it was reported that infarct volume or neuronal death were not affected (Le Feuvre et al., 2002). The lack of favorable effects of genetic ablation of the receptor may be due to the interplay of compensatory mechanisms. Surprisingly, we also report that activation using the most potent agonist of the receptor, BzATP, does not exacerbate the consequences of ischemic stroke. It could be speculated that BzATP could not further activate the receptor, since it was already activated by excess ATP in the extracellular space due to ischemic injury. In fact, a feedback control of the receptor could be surmised from the observations that activation of the receptor either by ATP or another agonist led to phosphorylation (Kim et al., 2001) and eventually redistribution between plasma membrane and cytosol (Feng et al., 2005). In addition, the receptor's unusually long C-terminal and extracellular loop between two transmembrane domains might also allow such feedback controls.

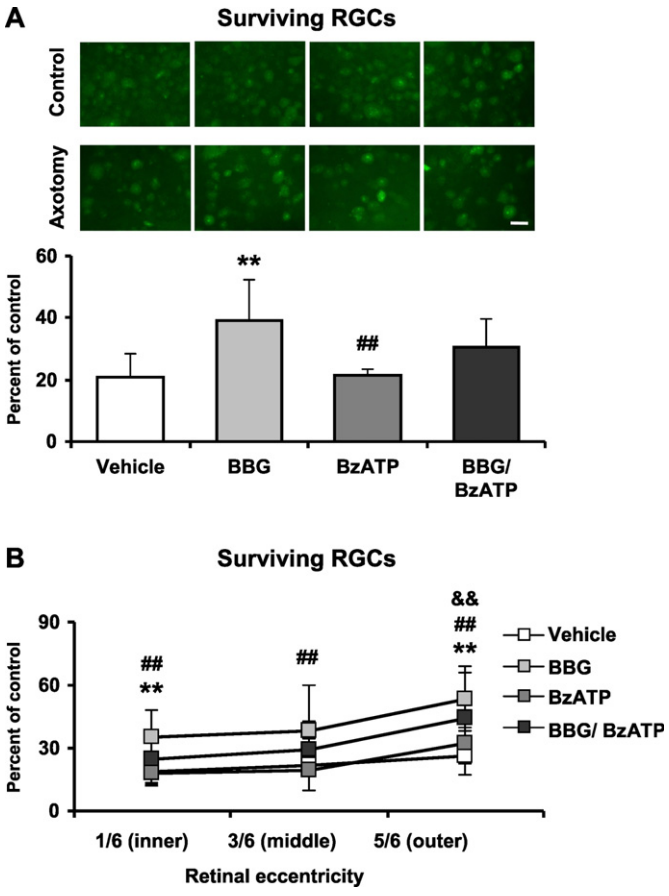

Fig. 5. P2X7R blockage protects axotomized RGCs from retrograde degeneration. Survival rates of fluorogold-prelabeled RGCs in mice following optic nerve (ON) transection were evaluated after 14 days and averaged over the whole retina (A) and also at various retinal eccentricities (B). BBG significantly increased neuronal survival in the retina following ON transection. However BzATP and vehicle did not result in any difference in neuronal survival. Data are mean values ± S.D. (n = 7 animals/group). (A) $^{**}p < 0.01$ compared with vehicle; $^{\#\#}p < 0.01$ compared with BBG treatment. (B) $^{**}p < 0.01$ vehicle vs BBG treated group, $^{\#\#}p < 0.01$ BBG vs BzATP treated group. $^{\&\&}p < 0.01$ BzATP vs BBG/BzATP treated group. Scale bar equals to 50 μm.

Although the expression profile of P2X7R in the brain is controversial, there are reports indicating that it is predominantly expressed in the resting microglia (Melani et al., 2006; Yanagisawa et al., 2008). It is well-described in the literature that resting microglia are activated following injury to clear the cellular debris and damaged tissue (Nimmerjahn et al., 2005). P2X7R was reported to drive resting microglial cells into activated state (Monif et al., 2009) and in the P2X7R knockout mice, microglial response to ischemic injury was decreased (Kaiser et al., 2016). Here, we report that activation of P2X7R by BzATP resulted in the increase in the number of Iba1+ microglia in the ischemic striatum, while BBG showed a significant decrease. As BzATP-treated microglia was shown to provide protective factors to the neurons in a co-culture system (Suzuki et al., 2004), it may be possible that P2X7R activated microglia is involved in emergency mechanisms that have protective roles in response to injury in the brain.

Moreover, BzATP activated survival kinases AKT and ERK-1/2, both of which are known to take part in ameliorating the ischemic tissue loss (Kilic et al., 2005). Upon P2X7R stimulation, upregulation of AKT (Jacques-Silva et al., 2004) and ERK (Gendron et al., 2003) was shown in cultures of astrocytes or astrocytoma, respectively. However, to our knowledge, this is the first study to report the activation of these two kinases following the activation of P2X7 receptors by BzATP in vivo. Surprisingly, BzATP also results in a moderate increase in the levels of pJNK, which is known to be downregulated by pAKT (Ben-Ami et al., 2011). Several lines of evidence have suggested that activated JNK exacerbates the reperfusion injury following ischemic stroke (Borsello et al., 2003) and there exists an antagonistic mechanism and possibly a balance between JNK and AKT/ERK survival pathways with the same downstream targets but differential consequences (Kamada et al., 2007). Therefore, increase in pJNK levels may partially be responsible for the lack of neuroprotective effects of increased pAKT levels by BzATP stimulation.

It should also be noted that during ischemia, sustained and progressive increase in extracellular ATP levels has long been known (Bai and Li, 2013; Dirnagl et al., 1999). Increased extracellular ATP, and subsequent increase in the levels of adenosine due to the conversion of

ATP by ecto-enzymes in the ischemic brain is probably so high that it can activate all purinergic receptor subtypes, including A1 receptors by adenosine that are known to provide protective effects in the affected region (Melani et al., 2012). Although reported in vitro (Kukley et al., 2004), whether extracellular BzATP is degraded to AMP and adenosine by ecto-nucleotidases in vivo in mice and that this degradation has a role in BzATP's non-deleterious effects should be addressed in future studies. Notably, ATP (and BzATP) was also suggested to promote neuroprotection independent from conversion into adenosine; however, this neuroprotection required the presence of microglial activity through P2X7R (Masuch et al., 2016).

Even though the protein expression data had a tendency towards protection resulting from BzATP stimulation, neuronal survival, infarct volume and motor function assays strongly indicated that it has neither protective nor detrimental effects on these parameters. Although the situation might be more complex, here we propose two likely mechanisms accounting for the inability of BzATP to translate the positive signaling pathways into positive outcomes. One mechanism involves the induction of P2X7R-mediated inflammation by BzATP. It was reported that brain ischemia resulted in increased IL-1β expression in neurons and in microglial cells (Minami et al., 1992) as well as increased IL-1β maturation and release following caspase1 activation (Le Feuvre et al., 2002). Indeed, we demonstrated that BzATP significantly increases IL-1β and cleaved caspase1 protein levels. The second mechanism involves secondary messenger mechanisms, namely intracellular Ca^{2+} overload. During ischemia, glutamate is released to the extracellular space and consequently increases Ca^{2+} overload via different mechanisms (Dirnagl et al., 1999). Consistent with this observation, we simulated it in the in-vitro condition by using primary neuron cultures under glutamate exposure and showed that BzATP results in a marked increase in Ca^{2+} influx. Considering the role of JNK and AKT/ERK survival pathways in secondary cell damage following increased intracellular Ca^{2+} levels (Haeusgen et al., 2009), it can be suggested that BzATP-mediated activation of AKT/ERK and JNK pathways may favor cell death in our injury models, and may be the reason why neither negative nor positive effect on survival could be observed with BzATP.

On the other hand, it is safe to suggest that the neuroprotective effect observed with BBG treatment is not mediated through the activation of survival kinase machinery, instead different mechanisms and signaling pathways may be involved in this process, including Ca^{2+} influx-regulated signaling cascades. From the data presented here, we suggest that BBG-mediated neuroprotection involves cessation of intracellular Ca^{2+} overload. This, in turn, decreases endoplasmic reticulum stress, organelle damage and apoptosis and leads to neuronal survival in ischemic injury in mice. Indeed, we showed that BBG decreased DNA fragmentation, infarct volume, brain swelling and increased neuronal survival in both ischemia and optic nerve transection models. In addition, pannexin channels were reported to contribute to the ischemic damage by helping P2X7 receptors form pore structures in plasma membrane. Pannexin channels were also shown to be involved in Ca^{2+} conductance of P2X7 receptors and NMDA receptors (Gulbransen et al., 2012). In this regard, inhibition of pannexin-mediated P2X7 receptor pore formation by BBG may further contribute to the neuroprotective effects observed with BBG. These results suggest that BBG ceases the P2X7R-mediated inflammation, and may exert its neuroprotective effects partially through the inhibition of inflammation. On the other hand, BzATP mediated receptor activation appears to trigger inflammatory response, while downregulating apoptotic mechanisms.

In summary, we described the mechanisms involved in neuronal survival vs death through the activation or inhibition of P2X7 receptor following FCI in mice. Our results also emphasize the complex nature of P2X7 receptor-mediated signaling in neuronal injury, suggesting that the receptor is activated by a context-dependent manner and that while its inhibition promoted survival, its activation does not necessarily mean neuronal death following ischemic stroke and further studies should be conducted to investigate the possible role of BzATP in the induction of ischemic tolerance.

Conflict of interest

The authors declare that they have no conflict of interest.

Author contributions

This work was carried out in collaboration between all authors. U. Kilic and E. Kilic defined the research theme and G. Ozturk, and F. Sahin revised the manuscript critically. A.B. Caglayan, M.C. Beker, T. Kelestemur designed methods and experiments, carried out the animal experiments. M. Beker, B. Caglayan, E. Sertel and E. Yalcin, carried out western blot and wrote the manuscript. A.B. Caglayan, M.C. Beker and E. Kilic collected and analyzed the data, and interpreted the results.

Funding

This work was supported by Turkish Academy of Sciences (TUBA).

References

Bai, H.Y., Li, A.P., 2013. P2X(7) receptors in cerebral ischemia. Neurosci. Bull. 29:390–398. http://dx.doi.org/10.1007/s12264-013-1338-7.
Barreto-Chang, O.L., Dolmetsch, R.E., 2009. Calcium imaging of cortical neurons using Fura-2 AM. J. Vis. Exp. 23:1067. http://dx.doi.org/10.3791/1067.
Beker, M.C., Caglayan, A.B., Kelestemur, T., Caglayan, B., Yalcin, E., Yulug, B., Kilic, U., Hermann, D.M., Kilic, E., 2015. Effects of normobaric oxygen and melatonin on reperfusion injury: role of cerebral microcirculation. Oncotarget 6:30604–30614. http://dx.doi.org/10.18632/oncotarget.5773.
Ben-Ami, I., Yao, Z., Naor, Z., Seger, R., 2011. Gq protein-induced apoptosis is mediated by AKT kinase inhibition that leads to protein kinase C-induced c-Jun N-terminal kinase activation. J. Biol. Chem. 286:31022–31031. http://dx.doi.org/10.1074/jbc.M111.247726.
Bindra, C.S., Jaggi, A.S., Singh, N., 2014. Role of P2X7 purinoceptors in neuroprotective mechanism of ischemic postconditioning in mice. Mol. Cell. Biochem. 390:161–173. http://dx.doi.org/10.1007/s11010-014-1967-9.
Borsello, T., Clarke, P.G., Hirt, L., Vercelli, A., Repici, M., Schorderet, D.F., Bogousslavsky, J., Bonny, C., 2003. A peptide inhibitor of c-Jun N-terminal kinase protects against excitotoxicity and cerebral ischemia. Nat. Med. 9:1180–1186. http://dx.doi.org/10.1038/nm911.
Burnstock, G., 2007. Physiology and pathophysiology of purinergic neurotransmission. Physiol. Rev. 87:659–797. http://dx.doi.org/10.1152/physrev.00043.2006.
Denes, A., Lopez-Castejon, G., Brough, D., 2012. Caspase-1: is IL-1 just the tip of the ICEberg? Cell Death Dis. 3, e338. http://dx.doi.org/10.1038/cddis.2012.86.
Diaz-Hernandez, J.I., Gomez-Villafuertes, R., Leon-Otegui, M., Hontecillas-Prieto, L., Del Puerto, A., Trejo, J.L., Lucas, J.J., Garrido, J.J., Gualix, J., Miras-Portugal, M.T., Diaz-Hernandez, M., 2012. In vivo P2X7 inhibition reduces amyloid plaques in Alzheimer's disease through GSK3beta and secretases. Neurobiol. Aging 33:1816–1828. http://dx.doi.org/10.1016/j.neurobiolaging.2011.09.040.
Dirnagl, U., Iadecola, C., Moskowitz, M.A., 1999. Pathobiology of ischaemic stroke: an integrated view. Trends Neurosci. 22:391–397. http://dx.doi.org/10.1016/S0166-2236(99)01401-0.
Feng, Y.H., Wang, L., Wang, Q., Li, X., Zeng, R., Gorodeski, G.I., 2005. ATP stimulates GRK-3 phosphorylation and beta-arrestin-2-dependent internalization of P2X7 receptor. Am. J. Phys. 288:C1342–C1356. http://dx.doi.org/10.1152/ajpcell.00315.2004.
Gandelman, M., Peluffo, H., Beckman, J.S., Cassina, P., Barbeito, L., 2010. Extracellular ATP and the P2X7 receptor in astrocyte-mediated motor neuron death: implications for amyotrophic lateral sclerosis. J. Neuroinflammation 7:33. http://dx.doi.org/10.1186/1742-2094-7-33.
Gendron, F.P., Neary, J.T., Theiss, P.M., Sun, G.Y., Gonzalez, F.A., Weisman, G.A., 2003. Mechanisms of P2X7 receptor-mediated ERK1/2 phosphorylation in human astrocytoma cells. Am. J. Phys. 284:C571–C581. http://dx.doi.org/10.1152/ajpcell.00286.2002.
Gulbransen, B.D., Bashashati, M., Hirota, S.A., Gui, X., Roberts, J.A., MacDonald, J.A., Muruve, D.A., McKay, D.M., Beck, P.L., Mawe, G.M., Thompson, R.J., Sharkey, K.A., 2012. Activation of neuronal P2X7 receptor-pannexin-1 mediates death of enteric neurons during colitis. Nat. Med. 18:600–604. http://dx.doi.org/10.1038/nm.2679.
Haeusgen, W., Boehm, R., Zhao, Y., Herdegen, T., Waetzig, V., 2009. Specific activities of individual c-Jun N-terminal kinases in the brain. Neuroscience 161:951–959. http://dx.doi.org/10.1016/j.neuroscience.2009.04.014.
Hilgenberg, L.G., Smith, M.A., 2007. Preparation of dissociated mouse cortical neuron cultures. J. Vis. Exp. 10:562. http://dx.doi.org/10.3791/562.
Jacques-Silva, M.C., Rodnight, R., Lenz, G., Liao, Z., Kong, Q., Tran, M., Kang, Y., Gonzalez, F.A., Weisman, G.A., Neary, J.T., 2004. P2X7 receptors stimulate AKT phosphorylation in astrocytes. Br. J. Pharmacol. 141:1106–1117. http://dx.doi.org/10.1038/sj.bjp.0705685.

Kaiser, M., Penk, A., Franke, H., Krügel, U., Nörenberg, W., Huster, D., Schaefer, M., 2016. Lack of functional P2X7 receptor aggravates brain edema development after middle cerebral artery occlusion. Purinergic Signal 12 (3):453–463. http://dx.doi.org/10.1007/s11302-016-9511-x.

Kamada, H., Nito, C., Endo, H., Chan, P.H., 2007. Bad as a converging signaling molecule between survival PI3-K/Akt and death JNK in neurons after transient focal cerebral ischemia in rats. J. Cereb. Blood Flow Metab. 27:521–533. http://dx.doi.org/10.1038/sj.jcbfm.9600367.

Khakh, B.S., North, R.A., 2006. P2X receptors as cell-surface ATP sensors in health and disease. Nature 442:527–532. http://dx.doi.org/10.1038/nature04886.

Kilic, E., Kilic, U., Soliz, J., Bassetti, C.L., Gassmann, M., Hermann, D.M., 2005. Brain-derived erythropoietin protects from focal cerebral ischemia by dual activation of ERK-1/-2 and Akt pathways. FASEB J. 19:2026–2028. http://dx.doi.org/10.1096/fj.05-3941fje.

Kilic, E., Kilic, U., Wang, Y., Bassetti, C.L., Marti, H.H., Hermann, D.M., 2006. The phosphatidylinositol-3 kinase/Akt pathway mediates VEGF's neuroprotective activity and induces blood brain barrier permeability after focal cerebral ischemia. FASEB J. 20:1185–1187. http://dx.doi.org/10.1096/fj.05-4829fje.

Kilic, U., Kilic, E., Jarve, A., Guo, Z., Spudich, A., Bieber, K., Barzena, U., Bassetti, C.L., Marti, H.H., Hermann, D.M., 2006. Human vascular endothelial growth factor protects axotomized retinal ganglion cells in vivo by activating ERK-1/2 and Akt pathways. J. Neurosci. 26:12439–12446. http://dx.doi.org/10.1523/JNEUROSCI.0434-06.2006.

Kilic, U., Kilic, E., Matter, C.M., Bassetti, C.L., Hermann, D.M., 2008. TLR-4 deficiency protects against focal cerebral ischemia and axotomy-induced neurodegeneration. Neurobiol. Dis. 31:33–40. http://dx.doi.org/10.1016/j.nbd.2008.03.002.

Kim, M., Jiang, L.H., Wilson, H.L., North, R.A., Surprenant, A., 2001. Proteomic and functional evidence for a P2X7 receptor signalling complex. EMBO J. 20:6347–6358. http://dx.doi.org/10.1093/emboj/20.22.6347.

Kukley, M., Stausberg, P., Adelmann, G., Chessell, I.P., Dietrich, D., 2004. Ecto-nucleotidases and nucleoside transporters mediate activation of adenosine receptors on hippocampal mossy fibers by P2X7 receptor agonist 2′-3′-O-(4-benzoylbenzoyl)-ATP. J. Neurosci. 24:7128–7139. http://dx.doi.org/10.1523/JNEUROSCI.2093-04.2004.

Le Feuvre, R.A., Brough, D., Iwakura, Y., Takeda, K., Rothwell, N.J., 2002. Priming of macrophages with lipopolysaccharide potentiates P2X7-mediated cell death via a caspase-1-dependent mechanism, independently of cytokine production. J. Biol. Chem. 277:3210–3218. http://dx.doi.org/10.1074/jbc.M104388200.

London, A., Benhar, I., Schwartz, M., 2013. The retina as a window to the brain-from eye research to CNS disorders. Nat. Rev. Neurol. 9:44–53. http://dx.doi.org/10.1038/nrneurol.2012.227.

Marcellino, D., Suarez-Boomgaard, D., Sanchez-Reina, M.D., Aguirre, J.A., Yoshitake, T., Yoshitake, S., Hagman, B., Kehr, J., Agnati, L.F., Fuxe, K., Rivera, A., 2010. On the role of P2X(7) receptors in dopamine nerve cell degeneration in a rat model of Parkinson's disease: studies with the P2X(7) receptor antagonist A-438079. J. Neural Transm. 117:681–687. http://dx.doi.org/10.1007/s00702-010-0400-0.

Masuch, A., Shieh, C.H., van Rooijen, N., van Calker, D., Biber, K., 2016. Mechanism of microglia neuroprotection: involvement of P2X7, TNFα, and valproic acid. Glia 64 (1):76–89. http://dx.doi.org/10.1002/glia.22904.

Mathers, C.D., Boerma, T., Ma Fat, D., 2009. Global and regional causes of death. Br. Med. Bull. 92:7–32. http://dx.doi.org/10.1093/bmb/ldp028.

Melani, A., Corti, F., Stephan, H., Muller, C.E., Donati, C., Bruni, P., Vannucchi, M.G., Pedata, F., 2012. Ecto-ATPase inhibition: ATP and adenosine release under physiological and ischemic in vivo conditions in the rat striatum. Exp. Neurol. 233:193–204. http://dx.doi.org/10.1016/j.expneurol.2011.09.036.

Melani, A., Amadio, S., Gianfriddo, M., Vannucchi, M.G., Volontè, C., Bernardi, G., Pedata, F., Sancesario, G., 2006. P2X7 receptor modulation on microglial cells and reduction of brain infarct caused by middle cerebral artery occlusion in rat. J. Cereb. Blood Flow Metab. 26 (7):974–982. http://dx.doi.org/10.1038/sj.jcbfm.9600250.

Minami, M., Kuraishi, Y., Yabuuchi, K., Yamazaki, A., Satoh, M., 1992. Induction of interleukin-1 beta mRNA in rat brain after transient forebrain ischemia. J. Neurochem. 58:390–392. http://dx.doi.org/10.1111/j.1471-4159.1992.tb09324.x.

Monif, M., Reid, C.A., Powell, K.L., Smart, M.L., Williams, D.A., 2009. The P2X7 receptor drives microglial activation and proliferation: a trophic role for P2X7R pore. J. Neurosci. 29 (12):3781–3791. http://dx.doi.org/10.1523/JNEUROSCI.5512-08.2009.

Murrell-Lagnado, R.D., Qureshi, O.S., 2008. Assembly and trafficking of P2X purinergic receptors (review). Mol. Membr. Biol. 25:321–331. http://dx.doi.org/10.1080/09687680802050385.

Nadal-Nicolás, F.M., Galindo-Romero, C., Valiente-Soriano, F.J., Barberà-Cremades, M., deTorre-Minguela, C., Salinas-Navarro, M., Pelegrín, P., Agudo-Barriuso, M., 2016. Involvement of P2X7 receptor in neuronal degeneration triggered by traumatic injury. Sci Rep 6:38499. http://dx.doi.org/10.1038/srep38499.

Nagasawa, K., Escartin, C., Swanson, R.A., 2009. Astrocyte cultures exhibit P2X7 receptor channel opening in the absence of exogenous ligands. Glia 57:622–633. http://dx.doi.org/10.1002/glia.20791.

Nimmerjahn, A., Kirchhoff, F., Helmchen, F., 2005. Resting microglial cells are highly dynamic surveillants of brain parenchyma in vivo. Science 308 (5726):1314–1318. http://dx.doi.org/10.1126/science.1110647.

North, R.A., 2002. Molecular physiology of P2X receptors. Physiol. Rev. 82:1013–1067. http://dx.doi.org/10.1152/physrev.00015.2002.

North, R.A., Jarvis, M.F., 2013. P2X receptors as drug targets. Mol. Pharmacol. 83:759–769. http://dx.doi.org/10.1124/mol.112.083758.

Rodrigues, R.J., Tome, A.R., Cunha, R.A., 2015. ATP as a multi-target danger signal in the brain. Front. Neurosci. 9:148. http://dx.doi.org/10.3389/fnins.2015.00148.

Skaper, S.D., Debetto, P., Giusti, P., 2010. The P2X7 purinergic receptor: from physiology to neurological disorders. FASEB J. 24:337–345. http://dx.doi.org/10.1096/fj.09-138883.

Suzuki, T., Hide, I., Ido, K., Kohsaka, S., Inoue, K., Nakata, Y., 2004. Production and release of neuroprotective tumor necrosis factor by P2X7 receptor-activated microglia. J. Neurosci. 24:1–7. http://dx.doi.org/10.1523/JNEUROSCI.3792-03.2004.

Tewari, M., Seth, P., 2015. Emerging role of P2X7 receptors in CNS health and disease. Ageing Res. Rev. 24:328–342. http://dx.doi.org/10.1016/j.arr.2015.10.001.

Thrift, A.G., Cadilhac, D.A., Thayabaranathan, T., Howard, G., Howard, V.J., Rothwell, P.M., Donnan, G.A., 2014. Global stroke statistics. Int. J. Stroke 9:6–18. http://dx.doi.org/10.1111/ijs.12245.

Wang, Y., Kilic, E., Kilic, U., Weber, B., Bassetti, C.L., Marti, H.H., Hermann, D.M., 2005. VEGF overexpression induces post-ischaemic neuroprotection, but facilitates haemodynamic steal phenomena. Brain 128:52–63. http://dx.doi.org/10.1093/brain/awh325.

Yanagisawa, D., Kitamura, Y., Takata, K., Hide, I., Nakata, Y., Taniguchi, T., 2008. Possible involvement of P2X7 receptor activation in microglial neuroprotection against focal cerebral ischemia in rats. Biol. Pharm. Bull. 31:1121–1130. http://dx.doi.org/10.1248/bpb.31.1121.

Zhang, X., Zhang, M., Laties, A.M., Mitchell, C.H., 2005. Stimulation of P2X7 receptors elevates Ca^{2+} and kills retinal ganglion cells. Invest. Ophthalmol. Vis. Sci. 46:2183–2191. http://dx.doi.org/10.1167/iovs.05-0052.